40

ИНСТИТУТ ЯДЕРНОЙ ФИЗИКИ
СО АН СССР

NONDIPOLE RADIATION AT PLANAR CHANNELING OF POSITRONS: COMPARISON OF THEORY WITH EXPERIMENT

V.N.Baier, V.M.Katkov, V.M.Strakhovenko

ПРЕПРИНТ 81 - 139

Новосибирск

NONDIPOLE RADIATION AT PLANAR CHANNELING OF POSITRONS: COMPARISON OF THEORY WITH EXPERIMENT

V.N.Baier, V.M.Katkov, V.M.Strakhovenko

Institute of Nuclear Physics,
Novosibirsk 630090, USSR

A b s t r a c t

The experiments studying the radiation at planar channeling (plane (110)) of positrons with energy $\mathcal{E}$ = 4,6,10,14 GeV in a diamond and with energy $\mathcal{E}$ = 10 GeV in a silicon are analysed /5/. A theory based on the authors' earlier papers was used, and it proved to be in satisfactory agreement with experiment.

The radiation at planar channeling of relativistic particles in crystals has been widely discussed in recent years (see Refs. [1-3] and the references there). There has been carried out a number of experimental studies of this process whose results are qualitatively consistent with theory. At present a quantitative comparison of theory with experiment seems urgent.

In the present paper we discuss the experiments on radiation of high-energy positrons at planar channeling (plane (110)) in a diamond crystal [4] ($\mathcal{E}$ = 4-14 GeV) and in a silicon one [5] ($\mathcal{E}$ = 10 GeV). The radiation at such energies is nondipole. A general theory of radiation at a quasi-periodical motion of particles which is developed by the authors is convenient to describe the phenomena. For calculation of the radiation characteristics it is necessary to average the results of Ref. [6] over the transverse energy particle distribution. In the experiments [4,5] the crystal thickness ℓ is less than ℓ_d, where ℓ_d is the dechanneling length [1] determined as a length at which the r.m.s. angle of multiple scattering in the same amorphous medium becomes equal to the Lindhard angle: $\vartheta_c = \sqrt{2U_0/\mathcal{E}}$, where U_0 is the depth of the potential well of the channel. Since the multiple scattering of positrons in the channel is suppressed compared to an amorphous medium, the analysis that follows will be concerned with "thin" crystals in which the change of the transverse energy distribution during the channeling process may be neglected. That is why the radiation at the channeling manifests itself, in the most clear way, in the experiments under consideration.

In case of the relativistic transverse motion the frequency of the emitted photon is determined by the following equation (see, e.g., Ref. [6])

$$\omega' = \omega \frac{\varepsilon}{\varepsilon - \omega} = \frac{2\gamma^2 \omega_0 n}{1 + \gamma^2 \theta^2 + \rho/2} \qquad (1)$$

where $\omega_0 = \frac{2\pi}{T}$, T is the period of the transverse motion of a particle, n is the number of the emitted harmonic, $\gamma = \varepsilon/m$, θ is the emission angle with respect to a direction of the average velocity, $\rho = 2\gamma^2 \overline{v_\perp^2}$, $\overline{v_\perp^2}$ is the mean value of the squared transverse (to the average) velocity of the particle. At $\rho \ll 1$ the radiation is dipole [1]. In the case $\rho \sim 1$ (just this situation occurs in the experiments [4, 5]) one or a few first harmonics is emitted and the spectrum is concentrated in the range of frequencies $\omega \sim \omega_c$:

$$\omega_c = \frac{2\gamma^2 \omega_0}{1 + \rho/2} \qquad (2)$$

and $\omega_c/\varepsilon \sim \lambda_c/d \ll 1$ ($\lambda_c = 1/m$ is the Compton wavelength of the electron, d is the distance between the planes). The radiation may hence be described in terms of classic electrodynamics (we shall neglect the quantum corrections $\sim \omega/\varepsilon$).

The parameter ρ depends substantially on the integral of motion - the transverse energy of the particle, $\varepsilon_\perp = U(x) + \varepsilon v_x^2/2$. For example, for the oscillator potential

$$\frac{\rho}{\rho_0} = z + \vartheta(z-1)\left[\frac{\sqrt{z-1}}{\arcsin 1/\sqrt{z}} - \frac{2}{(\arcsin 1/\sqrt{z})^2}\right] \qquad (3)$$

where $\rho_0 = 2\gamma U_0/m$, $z = \varepsilon_\perp/U_0$. For particles in the channel ($\varepsilon_\perp < U_0$, label 'c') $\rho \backsim z$, ρ grows with increasing the transverse energy of the particle and reaches the maximum, $\rho = \rho_0$, at $\varepsilon_\perp = U_0$. At $z > 1$, when the particles move above the barrier ($\varepsilon_\perp > U_0$, label 'nc') and acquire a nonzero average velocity projection onto a direction normal to the corresponding plane, the quantity $\rho(z)$ decreases very fast, for example,

$$\rho_{nc}(z = 1.01) \simeq \rho_0/6.5 \qquad (4a)$$

and at $z \gg 1$

$$\rho_{nc}(z) \simeq 2\rho_0/45z \qquad (4b)$$

Such behaviour of $\rho(z)$ enables one to calculate, at $\rho_0 \sim 1$, the emission characteristics of the above-barrier particles in a dipole approximation.

The frequency of positron radiation ω at a given value of the transverse energy $\varepsilon_\perp$ is ω_0- and ρ - dependent (1). In the dipole approximation ($\rho \ll 1$) the difference in emission frequencies (at a given θ, n) for various $\varepsilon_\perp$ is determined only by the $\varepsilon_\perp$-dependence of the motion frequency ω_0. For the oscillator potential there is no such dependence, and the spectral characteristic of the positron radiation with different values of the transverse energy differ by their intensity only. For this reason, if $\rho \ll 1$, the difference of the potential $U(x)$ from the oscillator one is essential even when the spread of frequencies ω_0 for the particles moving with various $\varepsilon_\perp$ is not too large (see Ref [1]). In the nondipole case ($\rho \gtrsim 1$), the more important factor determining the difference of the radiation frequencies for various $\varepsilon_\perp$ is the dependence of ω on $\rho(\varepsilon_\perp)$ and, hence, in this case the oscillator potential is suited as a rather good approximations.

The spectral density of the radiation intensity for the positron moving in the planar channel with a given $\varepsilon_\perp$ has the following form (see Ref [6], formula (4.8))

$$dI = \frac{2i}{\pi} e^2 \omega_0^2 \gamma^2 \xi d\xi \int_{-\infty}^{\infty} \frac{dt}{t} \exp\{-i\xi x_1\}. \qquad (5)$$

$$\cdot\left\{J_0(\xi x_0)+\rho\sin^2 t\left(J_0(\xi x_0)-i\,J_1(\xi x_0)\right)\right\}$$

where

$$\xi=\omega/2\omega_0\gamma^2\,,\quad x_0=\rho\left(\frac{\sin^2 t}{t}-\frac{\sin 2t}{2}\right),$$
$$x_1=2t\left[1+\frac{\rho}{2}\left(1-\frac{\sin^2 t}{t^2}\right)\right],\quad \rho=2\gamma\varepsilon_\perp/m \qquad (6)$$

The integration contour in (5) lies below the real axis. The integral (5) is a discontinuous function of $\xi(\omega)$ at the points $\xi(1+\rho/2)=2m+1$ ($m=0,1,2,\ldots$). It is possible to separate these jumps in an explicit form (see Ref.[6], formula (4.13)) and after that the remaining integral obtained is already a continuous function ξ, while the integrand behaves as $1/t^2$ at $t\to\infty$, that makes it convenient for numerical calculations.

Dividing (5) by $\omega=2\gamma^2\omega_0\xi$ and integrating it over ξ we find the total radiation probability:

$$W=\frac{2e^2\omega_0}{\pi}\int_0^\infty\frac{dt}{t}\left(\frac{1}{\sqrt{x_1^2-x_0^2}}+\frac{2\rho\sin^2 t}{\sqrt{x_1^2-x_0^2}+x_1+x_0}-\frac{1}{2t}\right) \qquad (7)$$

To obtain the radiation characteristics at channeling, the expressions (5) and (7) must be averaged over the transverse energy distribution. This procedure is identical to that in Ref.[1].

Let us turn now to a qualitative structure of the spectral intensity distribution at $\rho\sim 1$. In this case the largest portion of the radiation intensity comes from the first harmonic. Positrons radiate most effectively at $\varepsilon_\perp\simeq U_0$ so that, according to (2), the radiation (after averaging over the transverse energy distribution) attains a maximum at $\omega=\omega_{max}^{(1)}$, where

$$\omega_{max}^{(1)}=2\gamma^2\omega_0\xi_0\,,\quad \xi_0=1/(1+\rho_0/2) \qquad (8)$$

The minimum of the spectral density is on the boundary of the first harmonic:

$$\omega_{min}^{(1)}=2\gamma^2\omega_0\xi_1\,,\quad \xi_1=1/(1+\rho_1/2) \qquad (9)$$

where ρ_0 is defined in (3), ρ_1 is a value of ρ at as low as possible value of $\varepsilon_\perp$. For example, for the particles entering a crystal at an angle $\vartheta=\vartheta_0<\vartheta_c=\sqrt{2U_0/\varepsilon}$ to the crystal plane $z_1=\vartheta_0^2/\vartheta_c^2$, $\rho_1=\rho(z_1)$ (cf.(3)). The appearance of the second maximum in the spectral distribution is due to the contribution from the second harmonic of radiation, $\omega_{max}^{(2)}=2\omega_{max}^{(1)}$. Such a picture is clearly observed if $2\xi_0>\xi_1$. If the inverse inequality holds, the minimum of the averaged intensity lies (in terms of ξ) between the points ξ_0 and $2\xi_0$ and is to the left of the point ξ_1. In the particular case $2\xi_0\simeq\xi_1$ these structures can be washed out.*

For a given angle of entry of the particles into a crystal (ϑ), after averaging over the point of entry by means of formula (1.5) in Ref.[1], we obtain

$$\langle I_c(\vartheta)\rangle=A\int_{b^2}^1\frac{z\,dz}{2\sqrt{z-b^2}}=\frac{A}{3}\sqrt{1-b^2}\,(1+2b^2)\,\vartheta(1-b^2) \qquad (10)$$

for the total radiation intensity of positrons trapped into the channel, where $A=\frac{2}{3}\frac{e^2}{d^2}\rho_0^2$, $b=\vartheta/\vartheta_c$. Let the particles of

---

* Such a situation occurs, for example, at channeling of positrons with ε = 10 GeV and ϑ_0 = 0 in the plane (110) of the diamond and silicon single crystals; in this case, ρ_1 = 0 and $\rho_0/2\simeq 1$.

the incident beam are uniformly distributed over the angle ϑ in the interval $\vartheta_0 - \Delta \le \vartheta \le \vartheta_0 + \Delta$. Then the intensity (10) should be averaged over the angle ϑ .

$$\langle I_c(\tilde{\vartheta}_0, \tilde{\Delta})\rangle_\vartheta = \frac{A}{6\tilde{\Delta}} \int_{\tilde{\vartheta}_0 - \tilde{\Delta}}^{\tilde{\vartheta}_0 + \tilde{\Delta}} dx \sqrt{1-x^2}\,(1+2x^2)\,\vartheta(1-x^2) \qquad (11)$$

where $\tilde{\vartheta}_0 = \vartheta_0/\vartheta_c$, $\tilde{\Delta} = \Delta/\vartheta_c$. The quantity $\langle I_c(\tilde{\vartheta}_0, \tilde{\Delta})\rangle_\vartheta$ is an even function of ϑ_0 . In order to foreseen its behaviour at $\vartheta_0 = 0$, the secondary derivative is necessary to calculate. For $\tilde{\Delta} < 1$ we find

$$\left.\frac{\partial^2 \langle I_c(\tilde{\vartheta}_0, \tilde{\Delta})\rangle_\vartheta}{\partial \tilde{\vartheta}_0^2}\right|_{\tilde{\vartheta}_0 = 0} = A\,\frac{1-2\tilde{\Delta}^2}{\sqrt{1-\tilde{\Delta}^2}} \qquad (12)$$

At $\tilde{\Delta} < 1/\sqrt{2}$ the radiation intensity of the channelled positrons has the minimum at $\vartheta_0 = 0$ and vanishes when $\tilde{\vartheta}_0 = 1 + \tilde{\Delta}$, i.e. it has the maximum between these points. In the case of a wide beam, $\tilde{\Delta} > 1/\sqrt{2}$, the radiation intensity decreases with increasing ϑ_0 and it has the maximum at $\vartheta_0 = 0$. Thus, the behaviour of the radiation intensity as a function of the angle of entry depends, to a great extent, on the angular spread in the beam.

If the mean angle of entry of the particles $\vartheta_0 = 0$, the radiation intensity of positrons in the channel has the form

$$\langle I_c(0, \tilde{\Delta})\rangle_\vartheta = \frac{A}{4}\left\{\frac{\pi}{2\tilde{\Delta}}\,\vartheta(\tilde{\Delta}-1) + \right.$$
$$\left. + \vartheta(1-\tilde{\Delta})\left[\frac{\arcsin\tilde{\Delta}}{\tilde{\Delta}} + \frac{1}{3}\sqrt{1-\tilde{\Delta}^2}\,(1+2\tilde{\Delta}^2)\right]\right. \qquad (13)$$

This function has a minimum at $\Delta = 0$, reaches a maximum at $\tilde{\Delta} \simeq 0.77$, and decreases as $A\pi/8\tilde{\Delta}$ at $\tilde{\Delta} > 1$.

Since the calculation of the s[illegible]ral inte[illegible] turns out to be a fairly tedious [illegible]cedure, it seems usefu[illegible] find a

simple method for estimating the main maximum of this distribution when changing the magnitudes of ϑ_0 and Δ . Since this maximum position determined by formula (8) keeps unchanged, one can expect that its height will be connected with the total intensity of particles trapped into the channel. The numerical comparison has shown that these quantities are indeed related by a proportional dependence. The latter makes possible, starting with the quantity $d\langle I_c(\omega)\rangle/d\omega_{max}$ at fixed ϑ_c and Δ , to find the value of $d\langle I_c(\omega)\rangle/d\omega_{max}$ for any values of these parameters (we denote them via ϑ_{01} and Δ_1):

$$\left.\frac{d\langle I_c(\omega, \vartheta_{01}, \Delta_1)\rangle}{d\omega}\right|_{max} = \left.\frac{d\langle I_c(\omega, \vartheta_0, \Delta)\rangle}{d\omega}\right|_{max} \frac{\langle I_c(\vartheta_{01}, \Delta_1)\rangle}{\langle I_c(\vartheta_0, \Delta)\rangle} \qquad (14)$$

The above relation proves to be helpful in the analysis since it allows to compare the heights of the maximum of the spectral radiation distribution for various ϑ_0 and Δ by using the modified potentials. One of these modifications is, for example, a smoothing of the potential barrier on the channel's boundaries near the plane as a result of the lattice's zero and temperature vibrations. One can imitate this smoothing replacing the initial potential for a potential which is transformed, at a certain altitude, z_0 , into a "turned over" parabola whose maximum is at the point $x = d/2$. The corresponding data for such a modification are given in Table 1 in which the column with $z_0 = 1$ corresponds to a conventional parabola for which figures 9-13 are drawn for various values of parameter Δ .

The validity of the relation (14) is confirmed by direct comparison of these figures and the values $\langle I_c\rangle$ presented in the Table in arbitrary units.* The value $z_0 = 0.84$ cor-

* Formula (14) makes it possible to obtain the contribution

responds to a silicon crystal at room temperature, i.e. just at this altitude the potential changes compared to the statical case. It follows from the data in Table 1 that the height of the first peak grows with increasing the angular interval Δ from 20 μR to 60 μR; moreover, the temperature "smoothing" has no influence on this tendency and even at $\xi_0 \simeq 0.6$ this tendency is conserved.

In Ref.[4] the spectral radiation distributions have been measured for positrons with $\mathcal{E}$ = 4,6,10,14 GeV moving along the plane (110) of a diamond single crystal of thickness l = 80 μm. The angular divergence of the positron beam was $\Delta \leqslant 10\mu$R, and the accuracy of orientation of the crystal was 11.5 μR. We obtained for the plane (110) in the diamond*: U_0 = 27.5 eV (here account is taken of the lattice' vibrations leading to the decrease of U_0). In this case the Lindhard angle is

$$\vartheta_c = \sqrt{\frac{2U_0}{\mathcal{E}}} = 74 \left(\frac{10\,\text{GeV}}{\mathcal{E}}\right)^{1/2} \mu R \qquad (15)$$

so that the positron beam may be regarded as a narrow one at all energies used in the experiment. The effect of multiple

cont-ed

of the particles moving in the channel. To obtain the total height, the contribution of the above-barrier particles must be added. The calculation of the last contribution is significantly simpler due to the dipole approximation.

* In Ref.[1] the plane potential was calculated for all media with the use of the Thomas-Fermi approximation. However, the result for a diamond (Z = 6) may be only regarded as a rough estimate, so we have carried out the more exact calculation.

scattering may be ignored because the ratio of the crystal thickness l to the dechanneling length l_d* is as follows:

$$\frac{l}{l_d} \simeq \frac{2\pi l}{\alpha \rho_0 L_{rad}} \simeq 0.7 \left(\frac{4\,\text{GeV}}{\mathcal{E}}\right) \qquad (16)$$

In Ref.[4] (Fig.3) the spectral intensity of the positron emission at $\mathcal{E}$ = 10 GeV is shown as a function of the angle of entry of the particles with respect to the plane (110). Fig.1 demonstrates the result of the theoretical calculation for the values of ϑ_0 indicated in [4] and Δ = 10 μR. Curve 4 in Fig.1 is presented for ϑ_0 = 0. As one should expect, it has the maximum at the point ξ_0 (see eq.(8)) and there is no characteristic structure discussed above ($2\xi_0 \simeq \xi_1$). At ϑ_0 = 46 μR (curve 3) the first and second maxima are at the points $\xi = \xi_0$ and $\xi = 2\xi_0$, and the minimum is at the point ξ_1 ($2\xi_0 > \xi_1$, see (9)). Comparing curves 4 and 3, one can see that the height of the peak elevates in accordance with the above analysis by means of formulas (14) and (11). Curve 1 and 2 in Fig.1 are calculated for the values of ϑ_0 equal to 115 and 92 μR, and if Δ = 10 μR the positrons are not trapped into the channel and all the emission is due to the above-barrier particles. At the same time, the experimental data of Ref.[4] (see our Fig.2) show the distinct peak at $\xi = \xi_0$ for ϑ_0 = 92 μR. This peak can manifest itself only during emission by positrons moving in the channel. The contribution of these particles remains substantial in the experiment even at ϑ_0 = 115 μR.

* It should be borne in mind that this estimate overstates the role of multiple scattering for positrons moving in the channel.

Thus one can conclude that there exists a significant (in ϑ_c units) effective angular spread when the positron beam travels through a diamond crystal.* This may be caused by the irregularity of the crystal structure (the so-called mosaic structure). The crystal used in the experiment [4] could have a mosaic structure larger than $50\mu R$ (Miroshnichenko, private communication). We have performed a detailed comparison of the theory with the experimental data available for various values of Δ. The accordance turns out to take place at $\Delta \simeq \vartheta_c$. Fig.2 demonstrates the curves for $\Delta = 75\mu R$. As it is seen in Fig.2, at this value of Δ the theory describes quite well the behaviour of the spectral intensity of radiation against ϑ_0. With this value of Δ we have calculated the spectral intensity distributions measured in [4] for $\vartheta_0 = 0$. Figures 3-6 show the experimental data for the spectral radiation intensity which have been obtained by the authors of Ref.[4] for $\mathcal{E} = 4;6;10;14$ GeV and for $\vartheta_0 = 0$. To compare the theoretical and experimental shapes of the spectra, the vertical scale of the theoretical curves was decreased by a factor of k. The theoretical predictions turned out to exceed, in absolute magnitude, the experimental ones; and for all energies $k \simeq 3$ (with an accuracy better than 10%) figures 3-6 also show the theoretical curves obtained for $\vartheta_0 = 0$ and $\Delta = 75\mu R$ ($k = 3$). It is seen that the theoretical shape of the spectra is consistent satisfactorily with

* This is also confirmed with the behaviour of the intensity with an increase of the angles of entry (cf. (11)-(14) and the analysis there).

** For energies $\mathcal{E} = 4;6$ GeV it was taken the other frequency scale on the theoretical graphs: $\omega = 0.8\,\omega_{theor}$

experiment. For the emission of positrons with $\mathcal{E} = 4;6$ GeV, when the contribution of the higher harmonics to the emission is relatively small and the boundary of emission of the first harmonic is to the left from the second maximum, a qualitative spectral structure is determined by formulas (8) and (9). At $\mathcal{E} = 10$ GeV the degeneration occurs: $2\omega^{(1)}_{max} = \omega^{(1)}_{min}$. Existence of the minimum and the second maximum at $\Delta = 75\mu R$ ($\Delta \simeq \vartheta_c$) is connected with the fact that in this case the weight of the states with $\varepsilon_\perp = 0$ in the transverse energy distribution is comparatively small. The structure of the spectrum at $\mathcal{E} = 14$ GeV corresponds also to the above theoretical analysis (see formulas (8) and (9)): at this energy $2\omega^{(1)}_{max} < \omega^{(1)}_{min}$, i.e. the first and second maxima corresponds to the emission of the corresponding harmonics and the minimum of spectral density is between them. It is worse to note that ϑ_c is decreased with increasing energy and at a given Δ the contribution of the above-barrier particles to the radiation becomes larger. The last is naturally taken into account in Figs.3-6. Moreover, the relative contribution of these particles is more significant at higher frequencies.

The experiment in Ref.[5] was dealt with the emission of positrons at an energy of 10 GeV during their passage through a silicon single crystal of thickness $l = 90\mu m$ along the plane (110). The depth of the potential well can be found from the results of Ref.[1]. With temperature vibrations taken into account we have $U_0 \simeq 25$ eV, and $\vartheta_c = 71\mu R$, $\rho_0 = 1.9$. If one estimates l_d, according to formula (1.6) in Ref.[1], then $l/l_d \simeq 1/4$. The distance between the planes (110) in Si is 1.92Å and the magnitude of $2\gamma^2\omega_0$ is found to be equal to approximately 110 MeV. In all graphs below, for $\mathcal{E} = 10$ GeV, for Si (110) frequencies are taken in units of $\xi = \omega / 2\gamma^2\omega_0$.

Fig.7 shows the theoretical graph and the experimental values (in arbitrary units) of the dependence of the number of emitted photons in the interval $30<\omega<80$ MeV against the angle of entry of positrons with respect to the plane (110). Since the radiation of the first harmonic has a maximum at frequency $\omega_{max}^{(1)} \approx$ 56 MeV (see formula (8)), this interval of photon energies corresponds to the characteristic radiation energies of the first harmonic by the positrons moving in the channel. In Fig.7 theory and experiment are consistent with each other, and the experimental values of $W(\vartheta_0)$ do not, at least, decrease with increasing $|\vartheta_0|$ up to $|\vartheta_0| \simeq 50\mu R$.

Similar data for photon energies in the interval $600<\omega<1000$ MeV are presented in Fig.8. The theoretical curve in Fig.8 was calculated according to the exact formulas, however, only the above-barrier positrons ($\varkappa > 3$) contribute to the radiation in the whole interval of angles ϑ_0. For such values of $\varkappa$ an approximation familiar as the coherent radiation theory becomes applicable* (see Ref.[7], p.83). In our opinion, the correspondence between the theoretical and experimental data in Fig.8 is unsatisfactory.

Figs. 9-18 show the theoretical spectral radiation intensities for various angles of entry of the positrons with respect to the plane (110). Figs. 9,14, and 16 show the experimental data [5], too. Just as in Ref. 4, we normalized the vertical scale, but in this case the experimental values on the graphs are increased by a factor of k, k = 1.2 in Fig.9 and k = 1.7 in Fig.

* The correspondence between the radiation theory at planar channeling and the theory of coherent radiation was discussed in Ref.[8]. In the case under consideration their predictions differ by a few per cent.

14 and k = 2 in Fig.16. The shapes of the theoretical curves and the positions of maxima and minima are in satisfactory agreement with experiment*. Note once more that for $\vartheta_0 = 0$ $2\omega_{max}^{(1)} \simeq \omega_{min}^{(1)} = 2\omega_0\gamma^2$ in these graphs and a position of minimum ceases to be connected with the lower boundary of the particle distribution over transverse energy. However, in the case when $\vartheta_{min} = 50\mu R$ (Fig.16), $2\omega_{max}^{(1)} > \omega_{min}^{(1)} = 2\omega_0\gamma^2\varepsilon_{1}$ (see eq.(9)) and $\varepsilon_1 = \varepsilon_0(\vartheta_{min}/\vartheta_c)^2 \simeq 0.95$ so that one can immediately indicate a position of minimum in the spectrum which corresponds to the radiation boundary of the first harmonic, $\omega_{min}^{(1)} \simeq 75$ MeV.

As for an absolute magnitude of the spectral intensity, the experimental and theoretical results are in agreement within their accuracy for the interval of angles $|\vartheta| < 20\mu R$ (Fig.9). The theoretical value of the absolute spectral intensity in the interval of angles $|\vartheta| < 50\mu R$ is larger than that in the interval $|\vartheta| < 20\mu R$ and, as it is shown above, the change of the shape of the potential due to temperature vibrations does not affect this tendency. Experimental data of the paper [5] indicate the opposite tendency, that contradicts, in our opinion, the data of the same experiment (see Fig. As has already been mentioned, radiation probability at lea does not decrease with increasing $|\vartheta|$ in the interval under discussion. Thus, theory exempt from free parameters describes satisfactorily a wide set of experimental results. One can hope that further experimental and theoretical studies will clear up the reasons for the rest discrepances.

We thank very much I.I.Miroshnichenko and a leader of experiment /5/ E.N.Tsyganov for numerous, detailed and extremely helpful discussions concerning the experimental situation.

* In Figs.11-13,15,17, and 18 the contribution of the above barrier particles is presented separately.

References

1. V.N.Baier, V.M.Katkov, V.M.Strakhovenko. Yadernaya Fizika, 33, 1284, 1981.
2. M.A.Kumakhov, Ch.G.Trikalinos. Phys.Stat.Sol (B) 99, 449,1980.
3. V.A.Basylev, V.I.Glebov, N.K.Zhevago. ZhETP, 78, 62, 1980.
4. I.I.Miroshnichenko, D.D.Myorri, P.O.Avakyan, T.X.Figut. Pis'ma v ZhETP, 29, 786, 1979.
5. N.A.Filatova et al. FERMILAB-PUB-81/34 exp., 1981.
6. V.N.Baier, V.M.Katkov, V.M.Strakhovenko. ZhETP, 80, 1348, 1981.
7. I.L.Ter-Mikaelyan. The influence of a medium on electromagnetic processes at high energies. Publishing House of the Armenian Academy of Sciences, Yerevan, 1969.
8. V.N.Baier, V.M.Katkov, V.M.Strakhovenko. Preprint INP 80-03, Novosibirsk, 1980.

Table I

	$Z_0 = 1$	$Z_0 = 0.84$	$Z_0 = 0.58$
$\|\vartheta\| < 20\mu R$	0.346	0.365	0.389
$\|\vartheta\| < 40\mu R$	0.376	0.394	0.413
$\|\vartheta\| < 60\mu R$	0.403	0.421	0.482
$\|\vartheta\| < 80\mu R$	0.347	0.362	0.423
$\|\vartheta\| < 100\mu R$	0.277	0.290	0.338

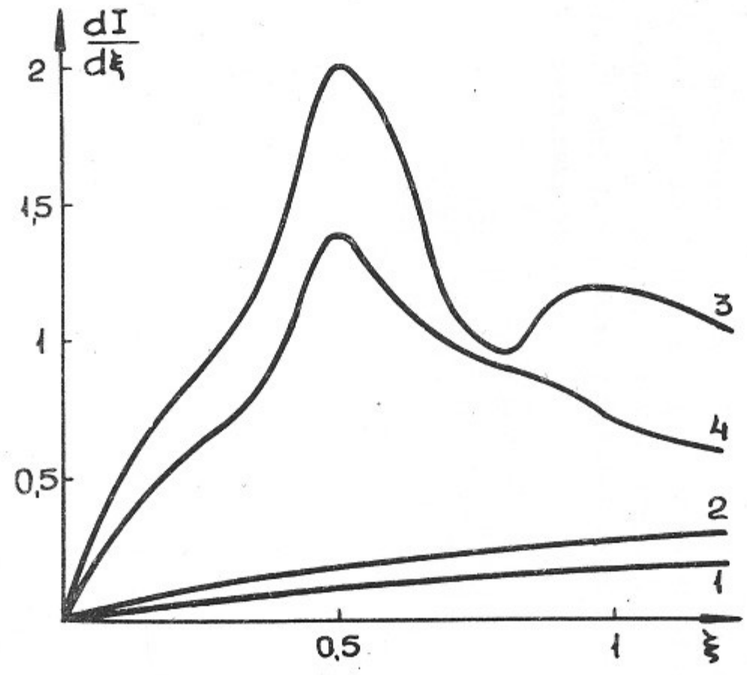

Fig.1. The radiation spectrum of positrons ($\mathcal{E}$ = 10 GeV. plane (110) in a diamond) in arbitrary units. Theoretical curves at Δ = 10μR: ϑ_0 = 115μR (curve 1), ϑ_0 = 92μR (curve 2), ϑ_0 = 46μR (curve 3), ϑ_0 = 0 (curve 4).

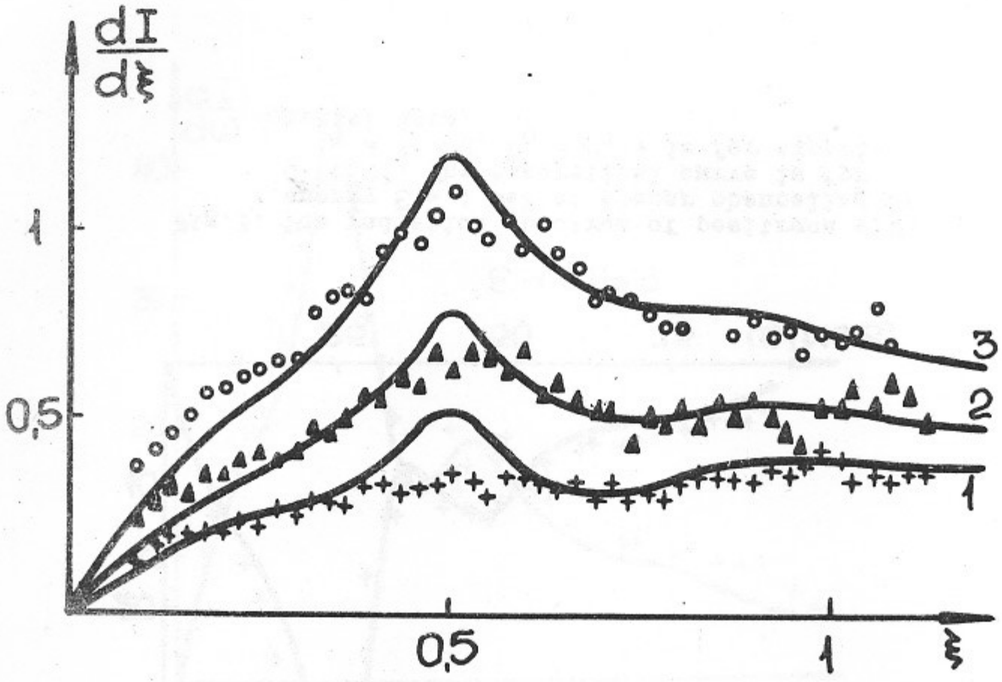

Fig.2. The spectral density of radiation intensity (in arbitrary units) at planar channeling of positrons with energy $\mathcal{E}$ = 10 GeV in plane C (110) as a functions of the angle ϑ_0 between the crystalline plane and the positron momentum. Experimental data [4] and corresponding theoretical curves for Δ = 75μR: o — ϑ_0 = 46μR (curve 3), ▲ — ϑ_0 = 92μR (curve 2), + — ϑ_0 = 115μR curve 1), ω = 178 MeV·ξ.

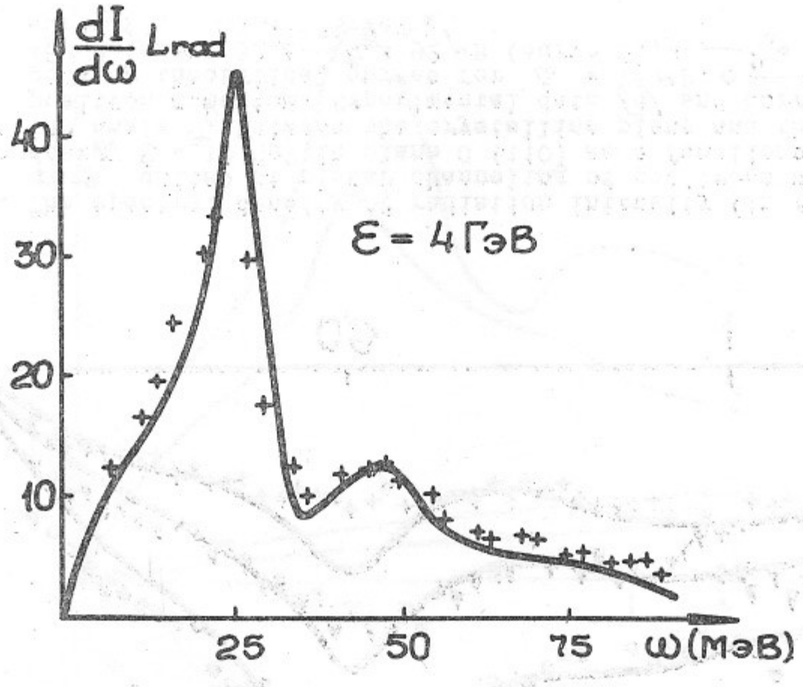

Fig.3. The radiation spectrum of positrons with energy $\mathcal{E}$ = 4 GeV at planar channeling in C (110). The theoretical curve is for Δ = 75 μR, ϑ_0 = 0, + is for experimental data.

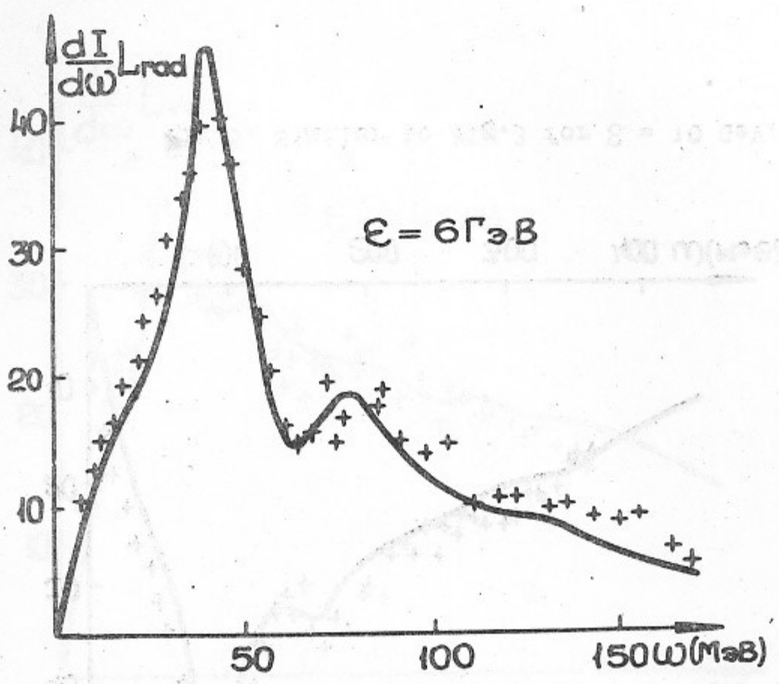

Fig.4. Similar to Fig.3 for $\mathcal{E}$ = 6 GeV.

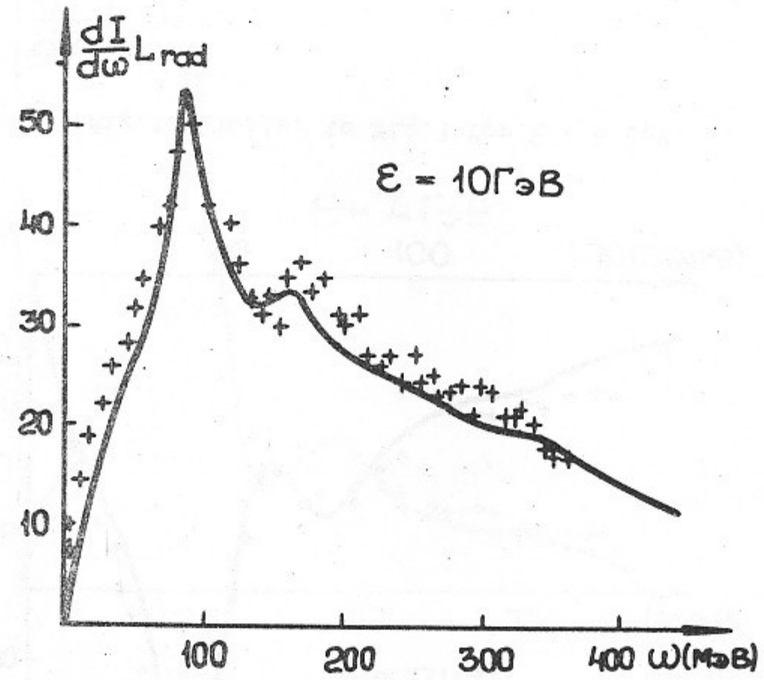

Fig.5. Similar to Fig.3 for $\mathcal{E}$ = 10 GeV.

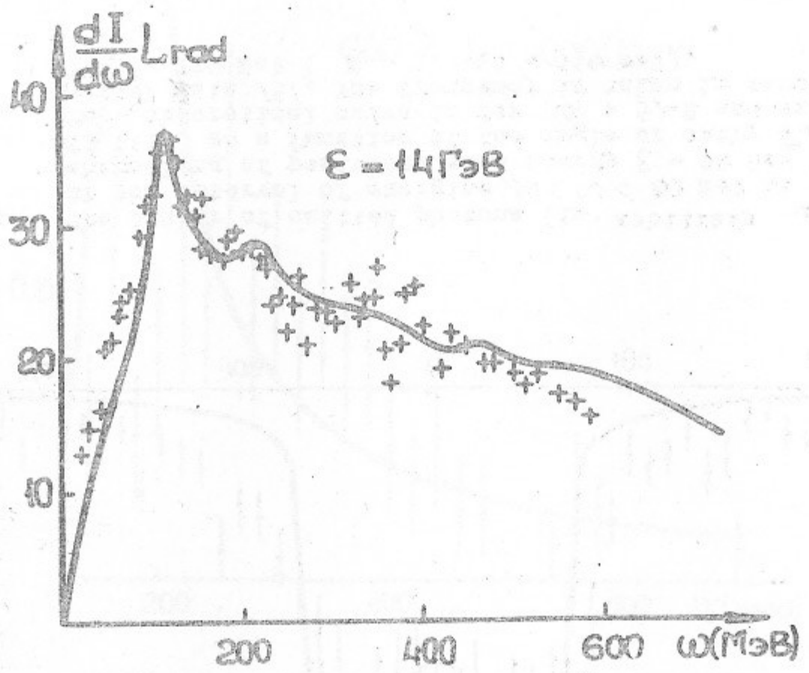

Fig.6. Similar to Fig.3 for $\mathcal{E}$ = 14 GeV.

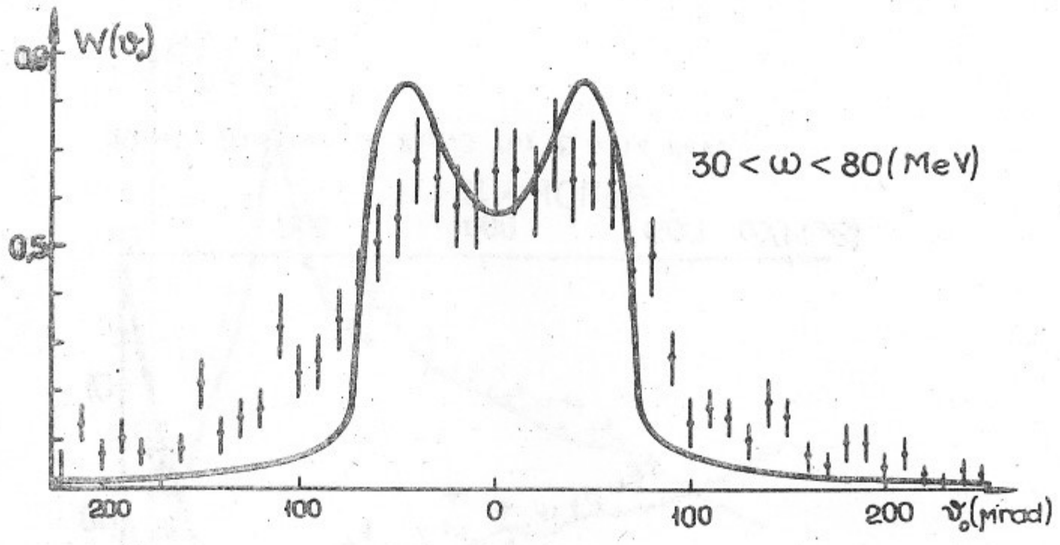

Fig.7. The number of emitted photons (in arbitrary units) in the interval of energies $30 < \omega < 80$ MeV at planar channeling of positrons with energy $\mathcal{E} = 10$ GeV in Si (110) as a function of the angle of entry ϑ_0. The theoretical curve is for $\Delta = 5\mu R$ and experimental data /5/. The frequency is taken in terms of $2\omega_0\gamma^2 = 110$ MeV ($\chi = 1$, $\omega = 110$ MeV).

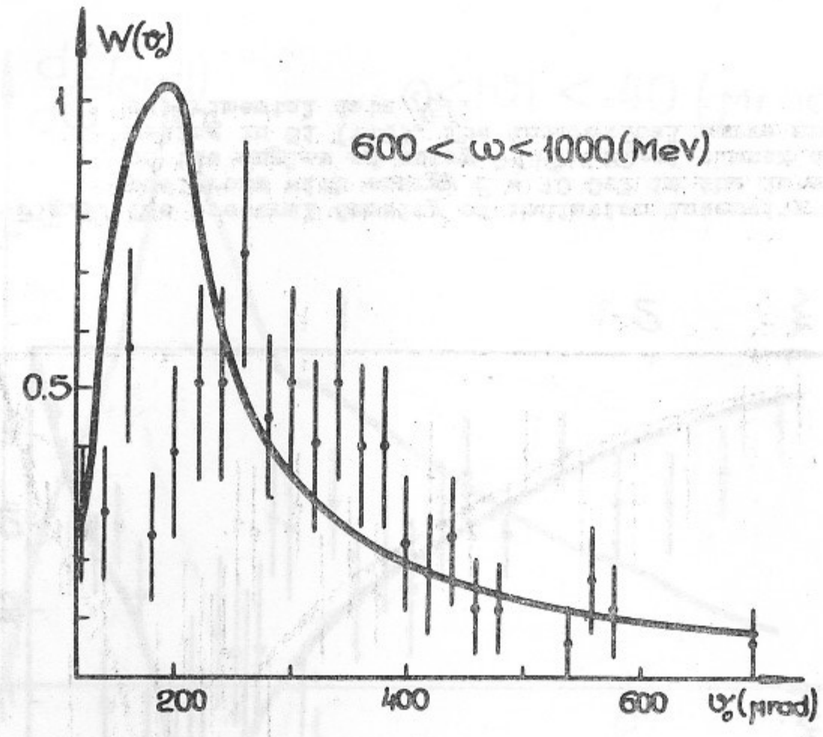

Fig.8. Similar to Fig.7 for $600 < \omega < 1000$ MeV.

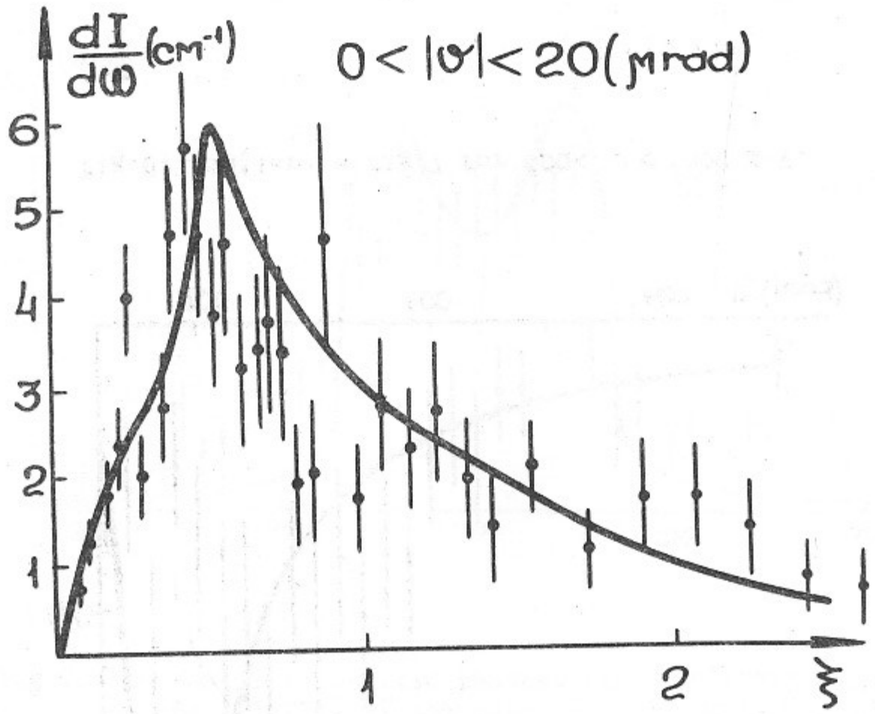

Fig.9. The spectral density of radiation intensity of positrons with energy $\mathcal{E}$ = 10 GeV in the interval of the angles of entry $0<|\vartheta|<20_{\mu R}$ at planar channeling in Si (110). The theoretical curve and experimental data [5].

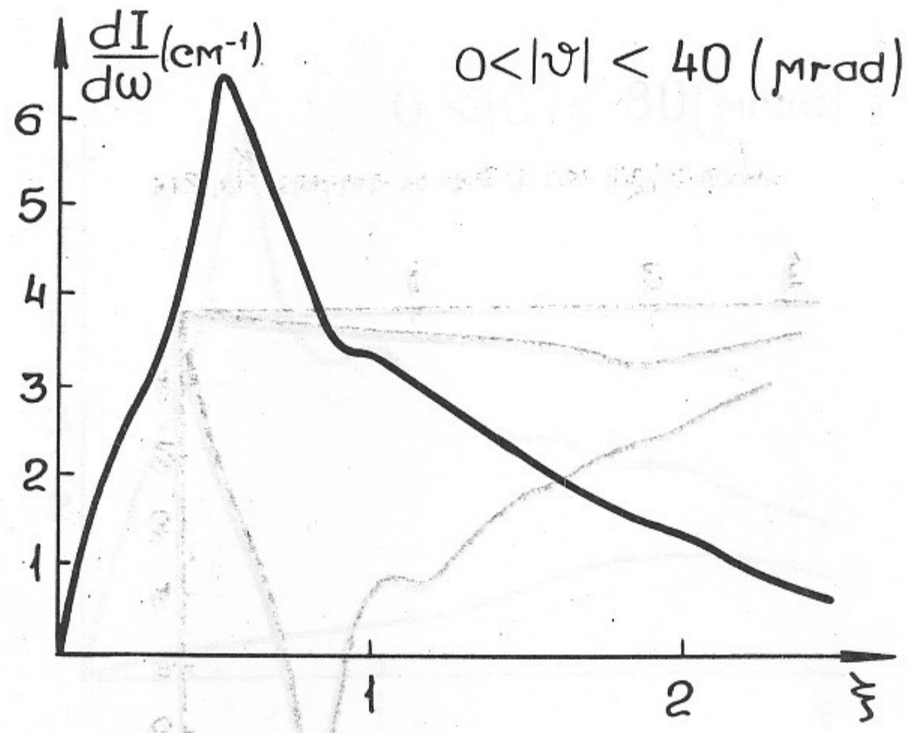

Fig.10. Similar to Fig.9 for $|\vartheta|<40\mu R$.

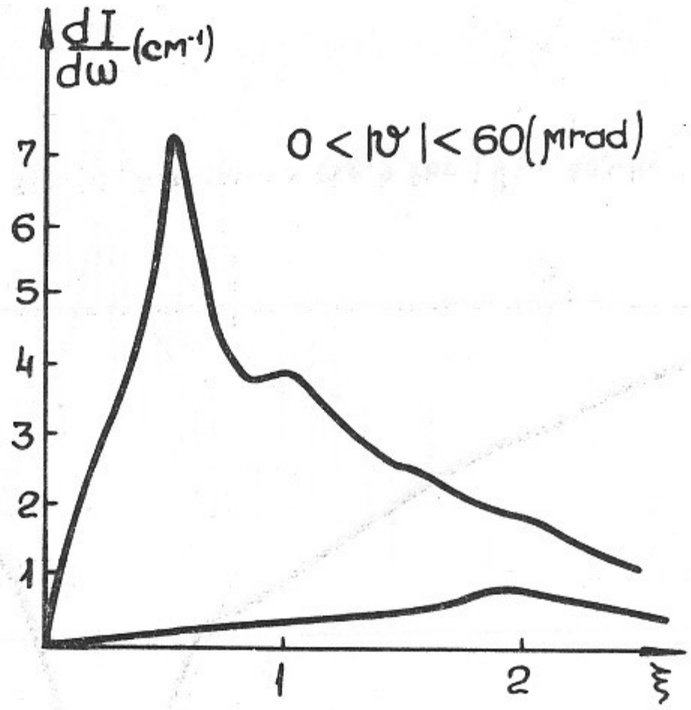

Fig.11. Similar to Fig.9 for $|\vartheta| < 60\mu R$.

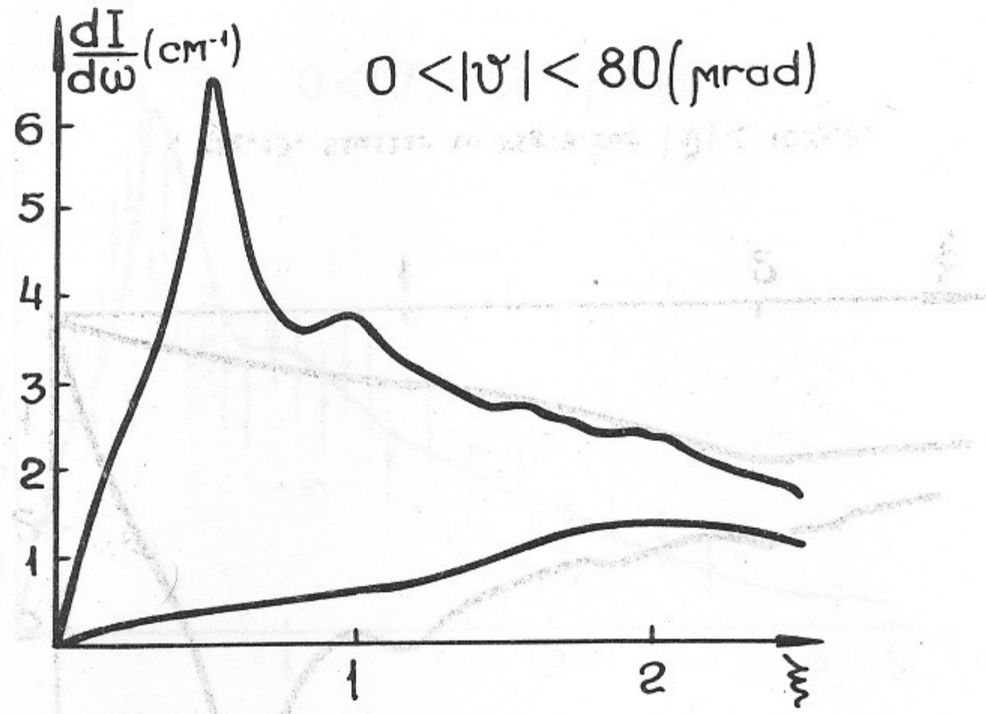

Fig.12. Similar to Fig.9 for $|\vartheta| < 80\mu R$.

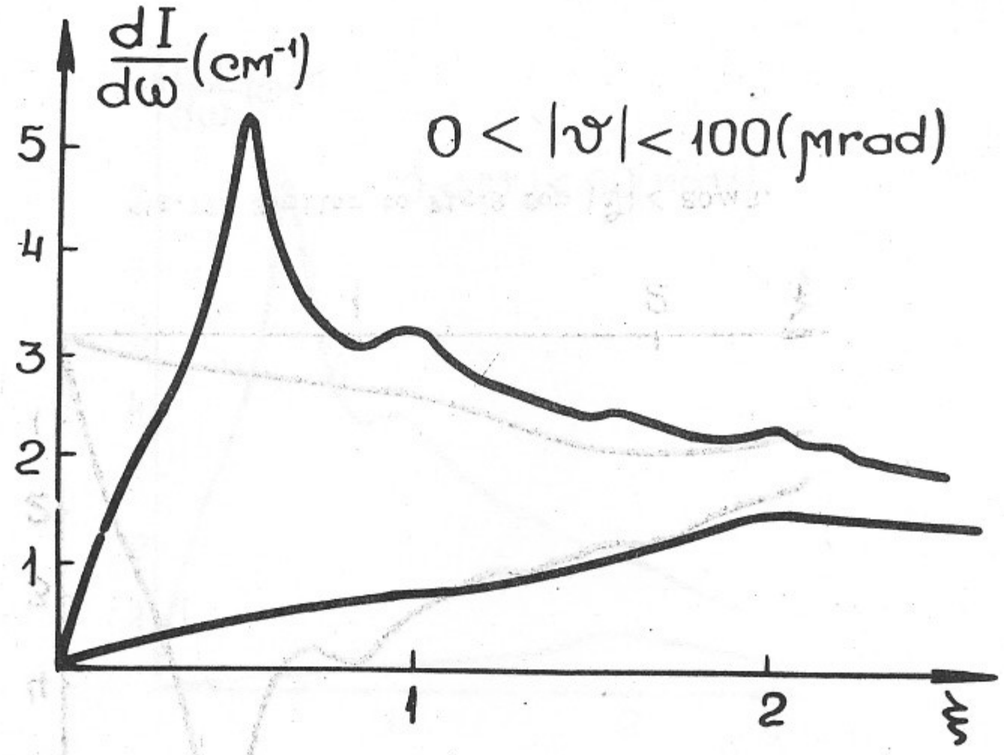

Fig.13. Similar to Fig.9 for $|\vartheta| < 100\mu R$.

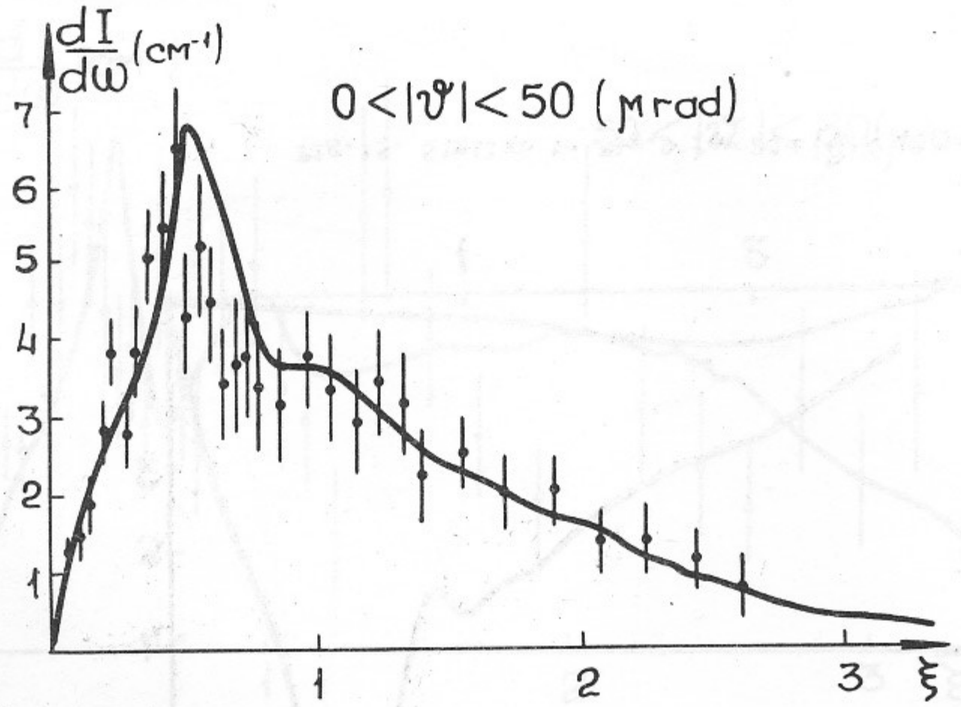

Fig.14. Similar to Fig.9 for $|\vartheta| < 50\mu R$.

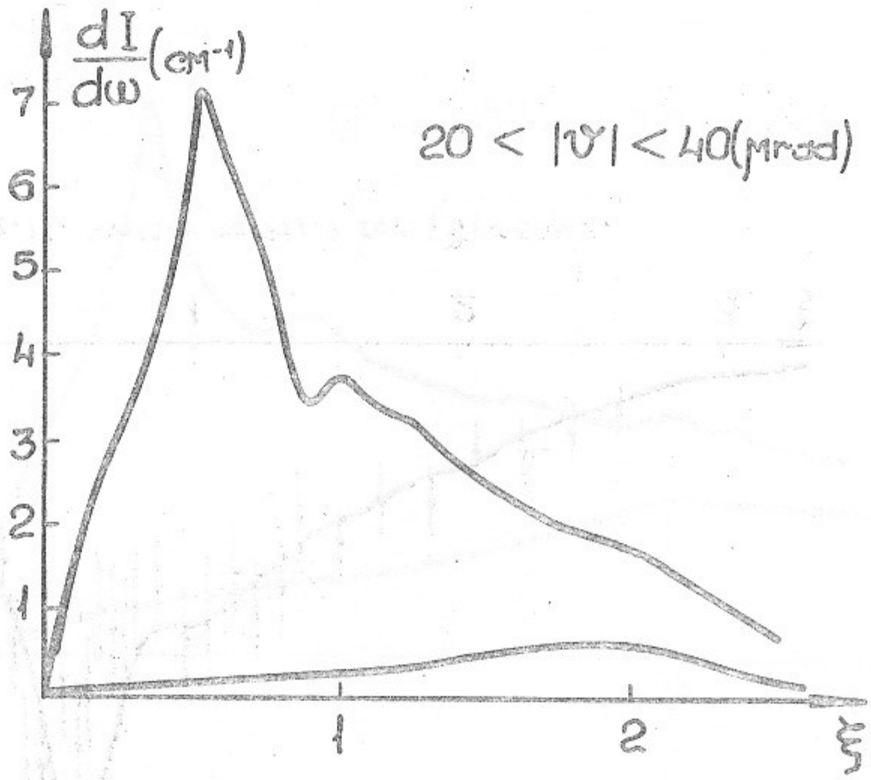

Fig.15. Similar to Fig.9 for $20<|\vartheta|<40\mu R$.

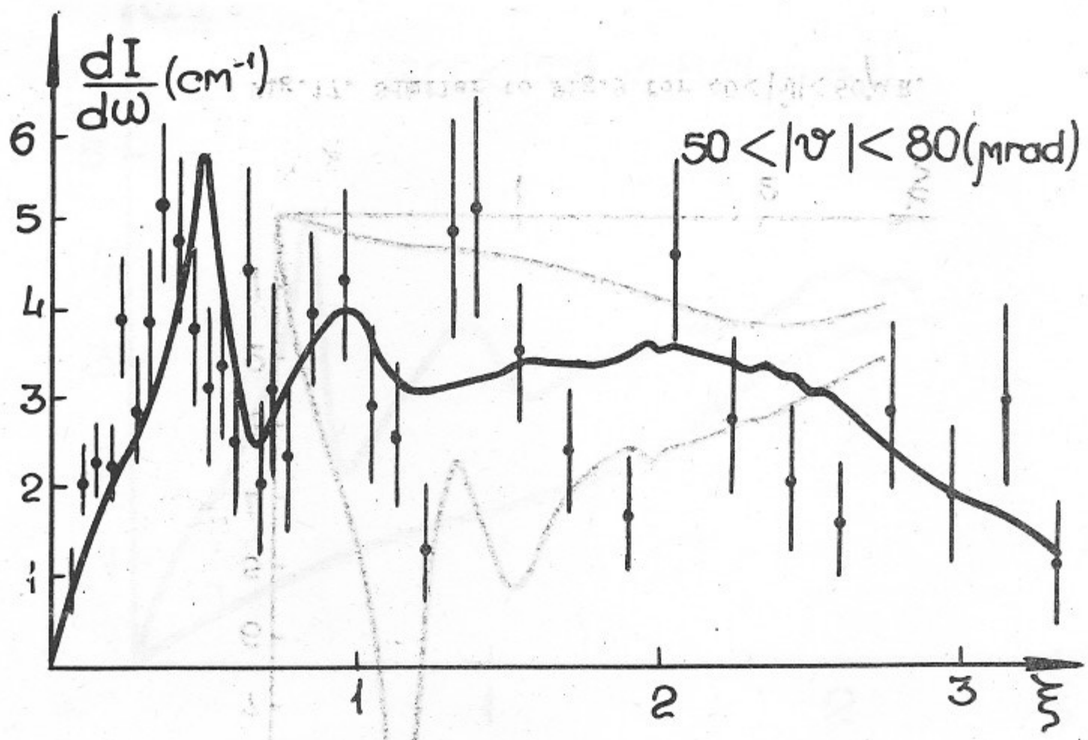

Fig.16. Similar to Fig.9 for $50<|\vartheta|<80\mu R$.

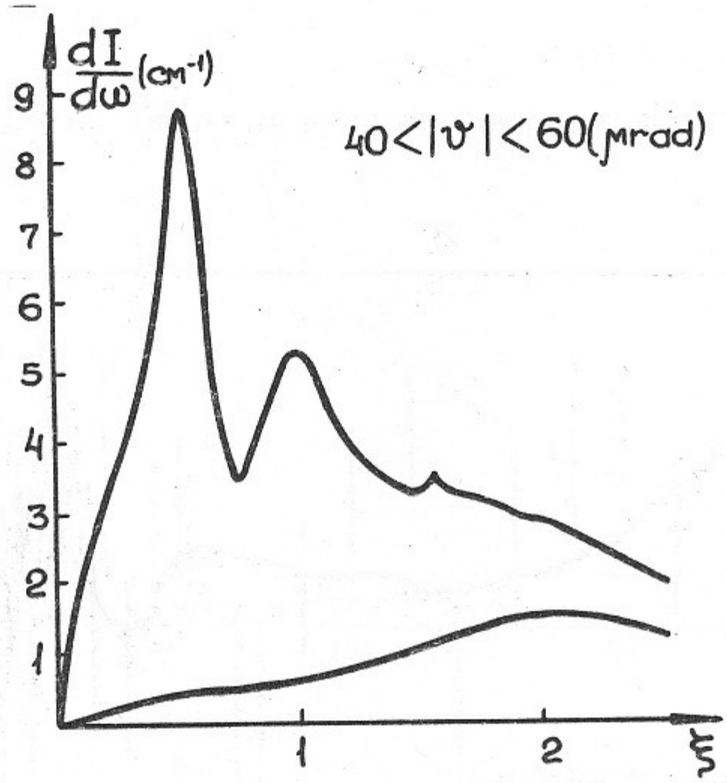

Fig.17. Similar to Fig.9 for $40<|\vartheta|<60\mu R$.

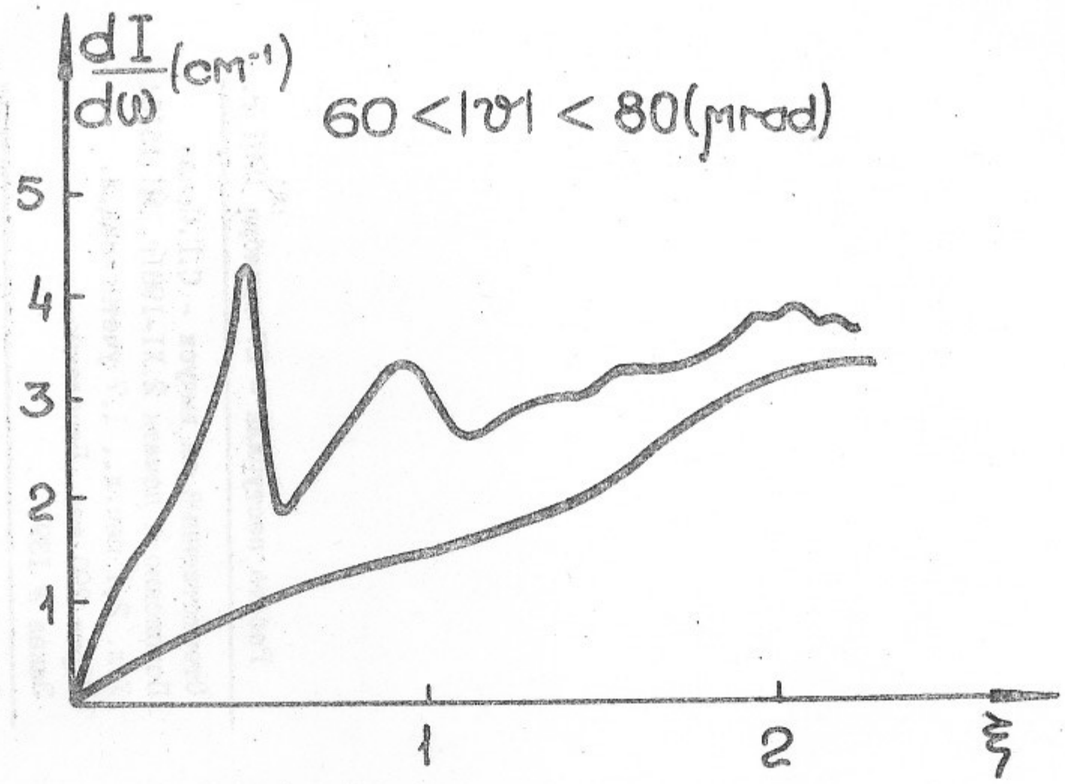

Fig.18. Similar to Fig.9 for $60<|\vartheta|<80\mu R$.

Работа поступила - 27 октября 1981 г.

Ответственный за выпуск - С.Г.Попов
Подписано к печати 2.XI-1981г. МН 15104
Усл. 2,1 печ.л., 1,7 учетно-изд.л.
Тираж 290 экз. Бесплатно
Заказ № 139.

Отпечатано на ротапринте ИЯФ СО АН СССР